

Ultraviolet and Multiwavelength Variability of the Blazar 3C 279: Evidence for Thermal Emission

E. Pian^{1,2,3}, C. M. Urry^{1,3}, L. Maraschi⁴, G. Madejski⁵, I. M. McHardy⁶, A. Koratkar¹,
A. Treves⁷, L. Chiappetti⁸, P. Grandi^{9,3}, R. C. Hartman⁵, H. Kubo¹⁰, C. M. Leach⁶,
J. E. Pesce¹, C. Imhoff^{1,11}, R. Thompson^{1,11}, A. E. Wehrle¹²

ABSTRACT

The γ -ray blazar 3C 279 was monitored on a nearly daily basis with IUE, ROSAT and EGRET for three weeks between December 1992 and January 1993. During this period, the blazar was at a historical minimum at all wavelengths. Here we present the UV data obtained during the above multiwavelength campaign. A maximum UV variation of $\sim 50\%$ is detected, while during the same period the X-ray flux varied by no more than 13%.

At the lowest UV flux level the average spectrum in the 1230-2700 Å interval is unusually flat for this object ($\langle\alpha_{UV}\rangle \sim 1$). The flattening could represent the

¹Space Telescope Science Institute, 3700 San Martin Drive, Baltimore, MD 21218

²Present address: Istituto di Tecnologie e Studio delle Radiazioni Extraterrestri, CNR, Via Gobetti 101, I-40129 Bologna, Italy

³Guest Observer with the *International Ultraviolet Explorer*

⁴Osservatorio Astronomico di Brera, via Brera 28, I-20121 Milan, Italy

⁵Laboratory for High Energy Astrophysics, Goddard Space Flight Center, Greenbelt, MD 20771

⁶Department of Physics, University of Southampton, Southampton SO9 5NH, UK

⁷Department of Physics, University of Como, Via Lucini 3, I-22100 Como, Italy

⁸Istituto di Fisica Cosmica e Tecnologie Relative, CNR, via Bassini 15, I-20133 Milan, Italy

⁹Istituto di Astrofisica Spaziale, CNR, via Fosso del Cavaliere, Area di Ricerca Tor Vergata, I-00133 Rome, Italy

¹⁰Department of Physics, Tokyo Institute of Technology, 2-12-1 Ookayama, Meguro, Tokyo 152-8551, Japan

¹¹Science Programs, Computer Sciences Corp., 1100 West Street, Laurel, MD 20707

¹²Infrared Processing Analysis Center, MC 100-22, Jet Propulsion Laboratory and California Institute of Technology, Pasadena, CA 91125

lowest energy tail of the inverse Compton component responsible for the X-ray emission, or could be due to the presence of a thermal component at ~ 20000 K possibly associated with an accretion disk. The presence of an accretion disk in this blazar object, likely observable only in very low states and otherwise hidden by the beamed, variable synchrotron component, would be consistent with the scenario in which the seed photons for the inverse Compton mechanism producing the γ -rays are external to the relativistic jet.

We further discuss the long term correlation of the UV flux with the X-ray and γ -ray fluxes obtained at various epochs. All UV archival data are included in the analysis. Both the X- and γ -ray fluxes are generally well correlated with the UV flux, approximately with square root and quadratic dependences, respectively.

Subject headings: galaxies: active — galaxies: blazars: individual (3C 279) — ultraviolet: galaxies — ultraviolet: spectra — X-ray: galaxies

1. Introduction

The blazar 3C 279 ($z = 0.538$) is a strong emitter at all energies, and one of the two brightest sources detected by EGRET in the γ -rays (Hartman et al. 1992; Wehrle et al. 1998; Mattox et al. 1997). Studies of its UV and X-ray emission (Bonnell, Vestrand, & Stacy 1993; Shrader et al. 1994; Koratkar et al. 1998; Makino et al. 1989) have detected remarkable variability on a range of time scales from days to years. Its UV spectrum exhibits strong, broad, high-ionization emission lines (Netzer et al. 1994; Koratkar et al. 1998), albeit not so luminous and broad as typically found in quasars, which makes this source intermediate between BL Lac objects and highly polarized quasars. The spectral energy distribution of 3C 279 has two broad humps peaked at far-infrared and MeV frequencies, and identified, according to the general interpretation of blazar continua, with synchrotron radiation and inverse Compton scattering, respectively, in a relativistic jet (Ulrich, Maraschi, & Urry 1997).

In the past few years, 3C 279 has been selected for simultaneous radio-to- γ -ray monitoring. The coordination of space- and ground-based observing facilities yielded the richest multiwavelength variability data ever obtained for a blazar (Maraschi et al. 1994; Hartman et al. 1996; Wehrle et al. 1998). The γ -ray emission, as observed also for other blazars (PKS 1622–297, Mattox et al. 1997; PKS 0537–441, Hartman 1996; Mkn 421, Macomb et al. 1995; Gaidos et al. 1996; Mkn 501, Catanese et al. 1997, Aharonian et

al. 1998; BL Lac, Bloom et al. 1997), exhibited the largest amplitude variability (up to a factor of ~ 100) within the electromagnetic spectrum on different time scales. However, these campaigns have not been able to determine the nature of the photons upscattered to the highest energies through the inverse Compton mechanism, and the origin of the γ -ray flares, a major puzzle of blazar physics.

Different scenarios have been proposed (see also Ghisellini & Maraschi 1996): the seed photons for the inverse Compton scattering can belong to an optical-UV radiation field internal to the jet (synchrotron photons; e.g., Maraschi, Ghisellini, & Celotti 1992) or external (accretion disk or broad emission line region; Dermer & Schlickeiser 1993; Sikora, Begelman, & Rees 1994). The latter might be viable in sources for which isotropic thermal and/or line emission is important, as compared with the beamed, non-thermal radiation. The strong emission lines observed in 3C 279 might provide the inverse Compton seed photons, which raises however a further question about the powering mechanism of the line emitting gas. The small variability of the Ly α emission line of 3C 279, at least on long time scales, points to a modestly variable ionizing source (Koratkar et al. 1998). This could be more likely a source of thermal origin, such as an inner disk, rather than the beamed radiation produced within the relativistic jet. In fact, if a jet illuminates the line emitting gas clouds, its beamed highly variable emission would produce rapid and large changes in the line flux, although only over a narrow velocity range. These could be responsible for the fast γ -ray continuum variations (Ghisellini & Madau 1996; Wehrle et al. 1998), however, short time scale (days or hours) line variability has been poorly studied, and never observed so far, in 3C 279.

The UV continuum of 3C 279 usually has a power-law shape and is rather steep, revealing its non-thermal origin. It is due to the radiation losses of the highest energy relativistic electrons injected in the jet. However, if the inverse Compton scattered photons are radiated from a disk, or from a broad line region powered by a disk, this component ought to be observed, at least when the synchrotron emission is quiescent. Therefore, 3C 279 in a low state is a good candidate for studying the underlying thermal emission component.

In this paper, we concentrate on the IUE monitoring of 3C 279 conducted during the EGRET observations in Phase 2 (December 1992-January 1993), when the source was in a low multiwavelength emission state, and Phase 3 (December 1993-January 1994). Some of the data were shown in Maraschi et al. (1994), Koratkar et al. (1998), and Wehrle et al. (1998). We present here the results of an improved, systematic analysis of the IUE data and compare them with X-ray results from the coordinated ROSAT PSPC and ASCA observations conducted during the EGRET pointings in Phases 2 and 3, respectively. The

X-ray data have been previously presented by Sambruna (1997, ROSAT) and Kubo et al. (1998, ASCA). Our independent re-analysis of these data yielded completely consistent results, therefore we refer the reader to those papers for a detailed description of the reduction and analysis.

In § 2 we present the IUE observations and data analysis, in § 3 we describe the UV spectral shape, also in relation to the simultaneous optical and X-ray data, and the light curves, and in § 4 we discuss these results and review the correlation of historical UV light curves of 3C 279 with the X-ray and γ -ray light curves.

2. IUE Data Acquisition, Reduction and Analysis

Low dispersion spectra of 3C 279 were taken, in both IUE wavelength ranges, 1230-1950 Å and 2000-3000 Å, from 1992 December 19 to 1993 January 10, and only at short wavelengths on 1993 December 24 and 25 (see Journal of Observations in Table 1). The source was in a very faint state, so that the signal was weak relative to the background. Inspection of the line-by-line LWP spectral images reveals contamination from solar scattered light longward of ~ 2750 Å (Caplinger 1995, and references therein). The NEWSIPS method for the spectral signal extraction, which has been adopted for the implementation of the IUE Final Archive, was modified to handle noisy, background-contaminated, low signal-to-noise ratio spectra. The extraction routine uses a default profile (point source in the present case) instead of the empirical cross-dispersion profile (Imhoff 1996). This avoids erroneous flux values for uncontaminated regions of the spectrum, and also minimizes the contribution of the spatially extended solar flux. Therefore, we used for our analysis the NEWSIPS extracted spectra. This extraction routine includes a camera head amplifier temperature correction and a time-dependent sensitivity degradation correction (see Nichols & Linsky 1996, and Garhart et al. 1997, where spectral flux calibration is also discussed). A recent improvement of the sensitivity degradation correction has been considered for the SWP spectra taken after January 1993 (Garhart et al. 1997; Garhart 1998; Imhoff 1997). For this reason, we re-analyzed also the two SWP spectra (53261 and 56635) of 3C 279 taken after the campaigns discussed in this paper (see Table 1). Cosmic rays in individual spectra were removed, and regions affected by camera artifacts were discarded (Crenshaw, Bruegman, & Norman 1990). We estimated the flux levels in the SWP and LWP spectra by averaging the signal in 200 Å-wide bands around the effective wavelengths of 1750 Å and 2600 Å for SWP and LWP spectra, respectively. These fluxes, along with their $1\text{-}\sigma$ uncertainties estimated as in Falomo et al. (1993), are reported in Table 1 and, after correction for Galactic reddening (see below), in Figure 1b (LWP only).

We have also compared our UV fluxes with those reported in Maraschi et al. (1994), using the same wavelength intervals and extinction value. While the SWP signal is consistent within the errors, the LWP signal reported earlier is almost a factor of 2 higher than presently found. We ascribe this discrepancy to the different spectral extraction. The method used by Maraschi et al. is likely to have significantly underestimated the solar light contamination, resulting in higher LWP source fluxes.

The expected interstellar extinction in the direction of 3C 279 due to Galactic neutral hydrogen is $A_V \simeq 0.13$ mag, corresponding to a column density $N_{HI} = 2.22 \times 10^{20}$ cm^{-2} (Elvis, Lockman, & Wilkes 1989), assuming a gas-to-dust ratio $N_{HI}/E_{B-V} = 5.2 \times 10^{21}$ cm^{-2} mag^{-1} (Shull & Van Steenberg 1985) and a total-to-selective extinction ratio $A_V/E_{B-V} = 3.1$ (Rieke & Lebofsky 1985). Pairs of SWP and LWP spectra taken close together in time were de-reddened with the extinction curve of Cardelli, Clayton, & Mathis (1989), and fitted to simple power-law models through an iterative, chi-squared minimization routine, by avoiding wavelengths dominated by Ly α emission at the redshift of the source (1850-1880 Å), the noisy regions shortward of 1230 Å and between 2000 and 2400 Å, and the wavelength interval longward of 2700 Å, which is contaminated by solar scattered light. The best-fit energy indices α_{UV} ($f_\nu \propto \nu^{-\alpha}$) are reported in Table 2, as are the reduced χ^2 values for each fit (χ_ν^2). A photometric uncertainty of 1.25% has been added in quadrature to the statistical error associated with each fitted flux (see Edelson et al. 1992).

The χ_ν^2 values for the power-law fits are generally not satisfactory. This is probably due to the fact that the errors associated with IUE spectral fluxes might be underestimated (see Urry et al. 1993). However, we tried instead fits with a black-body model to the merged spectra in the same wavelength interval used for the power-law fits. The results are reported in Table 2. The χ_ν^2 values are still not satisfactory, though systematically smaller than those associated with the power-law model fits. No fit to single SWP or LWP spectra was attempted because the former are too noisy for a reliable measurement of the spectral index, and for the latter the wavelength baseline is too narrow.

For comparison with the NEWSIPS method, we also retrieved and analyzed the spectra of 3C 279 of January 1993 extracted with the recently developed INES routine and available in the IUE archive at Vilspa (Loiseau & Schartel 1998). Power-laws have been fitted to the pairs of simultaneous SWP and LWP spectra after excluding the above wavelength intervals and de-reddening the data. The results are reported in Table 2.

The χ_ν^2 values obtained by fitting power-laws to INES extracted spectra are smaller than those of NEWSIPS spectra. We note however that spectral flux distributions derived from the INES extraction are systematically higher than the NEWSIPS, with differences

in the SWP spectra being marginally significant, and those in LWP spectra being much larger (up to 100%). This results in steeper spectral indices for fitted power-laws on average ($\langle\alpha_{UV}\rangle \simeq 1.5 \pm 0.2$, see Table 2), although still flatter than expected, based on the emission state (see §3.1 and cfr. with Table 3). The fact that the NEWSIPS LWP flux smoothly connects with the simultaneous optical data (Fig. 4) makes us suspect that the INES routine removes the contribution of the scattered light only partially, thus yielding significantly higher LWP fluxes than NEWSIPS does. Therefore, we prefer the NEWSIPS extraction. We also stress that at the present flux levels, slight differences in the background estimate either in the SWP or LWP camera can lead to dramatic differences in the extracted signal.

3. Results

3.1. The Ultraviolet Spectral Shape

The power-law fit to the quasi-simultaneous pairs of NEWSIPS extracted SWP and LWP spectra yields a much flatter energy index ($\langle\alpha_{UV}\rangle \simeq 1.0 \pm 0.2$) than generally measured in the 1230-3000 Å range for this source ($\langle\alpha_{UV}\rangle \simeq 1.5$; Webb et al. 1990; Edelson et al. 1992; Bonnell et al. 1994; Shrader et al. 1994). We investigated whether this can be ascribed to the more limited wavelength range used here (1230-2700 Å instead of 1230-3000 Å), or to a mismatch between the SWP and LWP spectra due to the NEWSIPS extraction routine or the calibration. To this purpose, we retrieved all the pairs of quasi-simultaneous (within ~ 1 day) NEWSIPS SWP and LWP spectra of 3C 279, fitted them jointly in the 1230-2700 Å interval, and compared our results (see Table 3) with those of the above authors (who used different extraction methods), finding a very good agreement. In the last line of Table 3 are reported the results of the fit to the joined simultaneous SWP and LWP spectra taken in the last IUE campaign of 3C 279 (Jan-Feb 1996, Wehrle et al. 1998), during which the UV flux was 3 times higher, which indicate a spectral slope steeper than those reported in the previous studies. We conclude the difference in spectral shape is real, not an artifact of the analysis. (Note that the extinction correction adopted here, $A_V = 0.13$, is the same as or higher than in previous analyses of the UV data. Therefore, to rule out de-reddening as a cause of spurious spectral flatness, we report in Table 3 the best-fit spectral indices for both observed and de-reddened spectra.) We also checked that no saturated spectra had been taken prior to each of our SWP exposures, which could have caused spurious residual flux adding up to the signal from 3C 279, and verified that the background in a region of the image very close to the object spectrum was not underestimated during spectral extraction. Although the signal-to-noise ratio of these

spectra is rather low, we find no instrumental explanation for the unusual flatness of the spectrum and so we conclude it has a physical origin.

In Figure 2 we show the available UV data (both from IUE and the HST Faint Object Spectrograph, FOS) of 3C 279, corrected for Galactic absorption and averaged, to increase the signal-to-noise ratio, according to flux level at the different epochs of observation (see caption). Superposed are the best fit power-law curves for each state. These fits show that the power-law slope flattens in the very low state of January 1993, as opposed to a general spectral steepening with decreasing flux seen at the other epochs, when the emission state was higher. The extremely low spectrum of January 1995 is also shown: it is similarly flat. Figure 3 shows the flux versus the spectral index for all the spectra in Figure 2. We have estimated the UV flux in a way independent of the fitted spectral index, to avoid introducing spurious correlation between the two quantities. For IUE spectra, the UV flux is the geometrical mean of the SWP signal at 1750 Å and the LWP signal at 2600 Å, therefore it refers to an effective wavelength of ~ 2130 Å. Uncertainties have been derived as in Edelson et al. (1992). For HST spectra, the flux at 2130 Å has been directly measured. The figure illustrates clearly the spectral steepening accompanying the flux decrease, and, at a flux of ~ 1 mJy, the reversal of this trend.

3.2. Comparison with the Optical Spectral Shape

To better characterize the spectral behavior of 3C 279 and elucidate the cause of the anomalous UV spectral flatness, we compared the UV data of January 1993 with optical BVRI photometry performed quasi-simultaneously (within ~ 12 hours) with the IUE observations (Grandi et al. 1996). In Table 2 we report the indices, along with χ^2_ν values, of power-laws fitted to the optical data only, optical and LWP, and optical, LWP and SWP. (For these fits, the UV data have been grouped in ~ 100 Å bins.) These parameters indicate that (1) the slopes of optical spectra are significantly steeper than those of the simultaneous UV spectra; (2) the indices of optical spectra are very similar to those of combined optical and LWP spectra, while (3) they are steeper than those of combined optical, LWP and SWP spectra. This suggests that the LWP spectra are consistent with the extrapolation of the optical to UV wavelengths, but that shortward of ~ 2000 Å a remarkable spectral flattening occurs.

The optical-UV spectral shape therefore suggests the presence of an emission component appearing at ~ 2000 Å superposed on that producing the optical and near-UV flux. One obvious candidate is thermal radiation from an inner accretion disk. Fitting the 1230-2700 Å flux distribution to a black-body model yields fit parameters for the four

spectra consistent at the $2\text{-}\sigma$ level (Table 2), and an average temperature of ~ 20000 K. Note that the black-body model fits have slightly smaller χ_ν^2 values than the power-law fits. However the very small difference, and the fact that χ_ν^2 values might be too high due to an underestimate of the IUE flux errors, do not allow us to select the correct model based only on the χ^2 . As a consistency check, black-body fits to the higher state average spectra reported in Figure 2 all give worse χ_ν^2 values than power-law fits.

3.3. Comparison with the X-ray Spectral Shape

We also explored whether the UV spectral flattening observed in January 1993 could have affected the simultaneously measured soft X-ray spectrum. The energy index for the ROSAT spectra in December 1992-January 1993 has an average $\langle\alpha_X\rangle = 0.85 \pm 0.05$ (0.1-2.4 keV), with very small variability (Sambruna 1997). ASCA observations one year later yield a significantly harder spectrum ($\langle\alpha_X\rangle = 0.65 \pm 0.07$ in the range 2-10 keV, with a $\chi_\nu^2 = 0.57$; Kubo et al. 1998) than the ROSAT one, but spectral variability between the two epochs is hard to assess, because of the difference in the energy ranges of the ROSAT and ASCA detectors, which are only partially overlapping. If temporal variability could be excluded, the observed difference would suggest that the spectrum hardens with energy in the 0.1-10 keV range. This is supported by the fact that the slope of the ASCA spectrum in the 0.7-10 keV energy range is 0.75 ± 0.03 , namely softer than between 2 and 10 keV. The average spectral change between the UV and X-ray simultaneous spectra in January 1993 is $\Delta\alpha \sim 0.2$. We also retrieved and analyzed the so far unpublished ASCA spectra of 3C 279 taken in December 1994-January 1995, obtaining a fitted spectral index $\alpha_X = 0.64 \pm 0.04$ ($\chi_\nu^2 \simeq 1$) in the 2-10 keV range. Including the softest energies in the fit (0.7-2 keV) does not result in a significantly different slope (the parameter N_{HI} was fixed at the Galactic value).

In the first four panels of Figure 4 we report the de-absorbed simultaneous optical-to-X-ray energy distributions of 3C 279 in January 1993, along with the black-body fit to the average IUE spectrum (fitted temperature $T = 20000 \pm 1000$ K, $\chi_\nu^2 = 0.8$). In the fifth panel we show a brighter state, for comparison, from the IUE-SWP and ASCA spectra in December 1993, and the average IUE-LWP spectrum of January 1996 (see caption to Fig. 2), which, albeit non-simultaneous with the SWP data, pertains to an emission state of similar level. No optical data at this epoch are available. The bright UV spectrum follows a power-law and any (flat) thermal component, if present at the level seen one year earlier, is not detectable.

3.4. Light Curves and Correlations

The UV flux at 1750 Å does not vary significantly during the first campaign (Jan 93), but increases by almost a factor of 3 the next year (Table 1). There is also a variation of $\sim 45\%$ between the latter two observations in December 1993. At longer UV wavelengths (2600 Å), for which sampling is available only during the first campaign, the flux varies day-to-day by 20-30%, if one excludes the $3\text{-}\sigma$ upper limit on 1992 December 27 (Fig. 1b). Including the upper limit, the maximum variation is more than 50% in a week. For comparison, the optical flux steadily increases during the monitoring by a factor 2.5 or more (Fig. 1a). The ROSAT light curve shows a $\sim 13\%$ amplitude flare of 2 days duration at the beginning of the campaign and a symmetric, larger (20% flux change from low to high state), slower ($\lesssim 10$ days including increase to maximum and decrease to initial state), and better sampled flare toward the end (Fig. 1c). An increase of $\sim 50\%$ is observed between the average ROSAT flux at 1 keV ($\sim 1 \mu\text{Jy}$, Sambruna 1997) and that recorded by ASCA one year later ($\sim 1.5 \mu\text{Jy}$, limiting the comparison to the soft energy band of ASCA, 0.5-2 keV).

We used the Discrete Correlation Function (DCF, Edelson & Krolik 1988) to study the correlation between X-ray emission and spectral slope during the ROSAT campaign (Fig. 2c and Table 2 of Sambruna 1997). The DCF amplitude curve (Fig. 5) has a minimum at a positive time-lag of $\sim 2\text{-}3$ days, suggesting that the flux increase leads the flattening of the spectral shape (hard lag).

4. Discussion

4.1. A Possible Thermal Origin of the Ultraviolet Radiation in the Low State

We have observed 3C 279 at UV wavelengths at two epochs separated by one year, simultaneously with X- and γ -ray observations. During the first epoch (Dec 92-Jan 93), the source was in one of its dimmest UV states ever. (The absolutely lowest state was reached in January 1995, see Table 1 and Fig. 2.) At the second epoch (Dec 93), the UV flux was a factor of 3 higher.

The archival IUE observations of 3C 279 suggest anticorrelation of the UV flux and spectral slope (flatter spectrum for brighter flux) at high or moderate emission levels, but the opposite behavior – positive correlation – at lower emission states. Indeed, at the lowest fluxes, the IUE spectral index is much flatter, $\langle \alpha_{UV} \rangle \sim 1$, than ever before seen. The high signal-to-noise ratio HST-FOS data support this reversal of trend, in that the 1992

spectrum, which corresponds to a lower state than that seen with the FOS in 1996, has also a slightly flatter slope. The flat slope of the IUE spectra can be fitted with a black-body model, with temperature $T \sim 20000$ K, but, because of the faintness of the source, it is impossible, based only on the goodness of the fits, to rule out a power-law model in favor of a black-body or other thermal (curved) model.

The optical spectrum is smooth and likely produced by synchrotron radiation (Grandi et al. 1996), with a slope $\alpha_{opt} \sim 1.8-2.0$. Thus, significant spectral flattening occurs in the UV range. If the UV spectrum were also due to the synchrotron mechanism it would imply a relativistic electron distribution that flattens sharply at higher frequencies whereas the electron distribution generally steepens progressively at higher frequencies due to radiative losses. Moreover, the optical flux varies with much higher amplitude than the UV (Fig. 1), which is also opposite to what is expected in a pure synchrotron model. It is possible that the flattening of the UV spectrum observed in the low state is due to a contribution of inverse Compton scattering extending to the UV wavelengths. However, the fitted temperature of the black-body model and the luminosity derived from the fitted normalization (see below) make it plausible that the low state UV spectrum is produced by thermal emission from an accretion disk with a temperature $T \sim 20000$ K. At soft X-ray energies the contribution of the black-body component falls off rapidly, and at 0.1 keV is negligible ($\sim 10^{-20}$ of the total flux), but one cannot exclude a significant contribution in the X-rays under the hypothesis of a more complex model, like a multi-temperature disk.

The spectral flattening observed in the 1230-2700 Å range at very low UV continuum levels, an uncommon feature in blazars, is typical of radio-quiet quasars. Quite plausibly it could be the signature of a thermal, quasi-isotropic component, perhaps a disk, which is normally swamped by the non-thermal, highly variable, beamed continuum of 3C 279. This “Seyfert-like” component would be visible in the UV only in very low states, namely when the contribution of the synchrotron radiation is less important. (The quality of the present UV data does not allow us to disentangle the two contributions by means of composite fits.) This could also explain the smaller variability observed in the UV than in optical light, under the assumption that the disk emission is not variable on time scales less than a few years. The observation of a still weaker flux in January 1995 at the shorter UV wavelengths (Fig. 2) suggests some yearly variability of this thermal component, albeit modest. Observation of wavelength dependent polarization in the UV could confirm the thermal interpretation if it is markedly different in the low state.

Assuming that a single black-body is a good approximation for the UV emission, and using the fit parameters obtained for the average IUE spectrum, at $z = 0.538$, with $H_0 = 65$ km s⁻¹ Mpc⁻¹ and $q_0 = 0.5$, the fitted normalization of the black-body corresponds to a

luminosity $L_{UV} \sim 2 \times 10^{45}$ erg s⁻¹ (if isotropic) and to a linear size of the emitting region of ~ 1 light day, consistent with the range of UV luminosities of typical quasars (Elvis et al. 1994) and with the inner dimensions of an accretion disk in an active galactic nucleus (Rees 1984), respectively. Theoretically, the presence of an accretion disk has been invoked as the hidden power source of the broad H α emission line in BL Lac (Corbett et al. 1996). The absence of intensity variations in the strong, broad Ly α emission line of 3C 279, as opposed to the high amplitude variability of the UV continuum, also argues for the presence of an accretion disk powering the broad line region (Koratkar et al. 1998). If this were the case, the UV photoionizing flux provided by our fitted black-body component ($\sim 1.4 \times 10^{-12}$ erg s⁻¹ cm⁻²) would account for the observed Ly α line intensity ($\sim 6.5 \times 10^{-14}$ erg s⁻¹ cm⁻²) assuming values normally expected in AGNs for the covering factor of the broad line clouds ($\sim 5\%$, e.g., Netzer 1990).

The fitted temperature of the black-body, 20000 K, implies an emission peak at rest frame wavelength ~ 1500 Å, in the range between the so-called “blue bump”, seen in quasars and interpreted as accretion disk emission, and the soft X-ray excess, exhibited by several Seyfert galaxies and generally identified as the high energy tail of the blue bump itself (see Kolman et al. 1993; Czerny & Elvis 1987; reviews by Bregman 1990 and 1994). A suggestion of an optical excess was found in a few blazars (Brown et al. 1989) and a blue bump has been clearly observed in at least one of them, 3C 345 (Bregman et al. 1986), in the radio-loud quasar 3C 273 (Shields 1975; Ulrich 1981), and in the radiogalaxy 3C 120 (Maraschi et al. 1991). For 3C 273 and for another radio-loud quasar, B2 1028+313, a soft X-ray excess has been detected (Masnou et al. 1992; Grandi et al. 1997; Haardt et al. 1998).

4.2. Multiwavelength Light Curves and Spectra

Multiwavelength variability (Maraschi et al. 1994; Hartman et al. 1996; Wehrle et al. 1998; Maraschi 1998) suggests that the broad-band spectrum of 3C 279 at radio-to-UV wavelengths and at X- and γ -ray energies is produced by synchrotron radiation and inverse Compton scattering, respectively. This is supported by the soft, power-law optical and UV continuum and by the flat spectra observed at medium and hard X-rays (Makino et al. 1989; Hartman et al. 1996; Kubo et al. 1998; Lawson & McHardy 1998). The spectral variability seen above ~ 2 keV is small, consistent with the fact that the X-rays are produced through inverse Compton scattering of relativistic electrons with small Lorentz factor, whose energy distribution slope is not expected to vary on short time scales. In fact, our analysis of the ASCA spectra of December 1994-January 1995 yields an energy index identical to or not

significantly different from those found at other epochs. The anticorrelation between UV flux and spectral index variations, predicted by models based on radiative cooling (Celotti, Maraschi, & Treves 1991), is instead consistent with a distribution of electrons with high Lorentz factor, which have more rapid radiative losses.

The soft X-ray spectrum appears more variable in the long term and it is softer for fainter flux (Schartel et al. 1996; Sambruna 1997), which might indicate that other radiation processes besides inverse Compton contribute in this spectral region, like, for instance, the high energy tail of the synchrotron component. Another possible candidate is thermal radiation. Although there is no sign in joint RXTE and ROSAT HRI data of a soft X-ray excess of thermal origin in this source (Lawson & McHardy 1998), the 0.1-2 keV spectrum measured by ROSAT in December 1992-January 1993 is steeper than that measured by ASCA in the 2-10 keV band in December 1993, which suggests the presence of an extra component at the lower energies, assuming no X-ray spectral variability between those two epochs. Moreover, in December 1993 the spectral slope in the range 0.7-10 keV was somewhat steeper than in 2-10 keV, which again points to the above suggestion.

Note that the soft X-ray flux variations precede those of the spectral index (Fig. 5), which is the contrary of what has been observed in other blazars, like Mkn 421 and PKS 2155–304, both in X-rays (Takahashi et al. 1996; Sembay et al. 1993; Treves et al. 1999; Chiappetti et al. 1999) and UV (Pian et al. 1997). In those sources the UV and X-ray emission is dominated by synchrotron radiation, and the variations at harder energies lead those at softer energies, which determines a lag of flux with respect to spectral index. In 3C 279 the non-thermal X-ray emission likely has a different origin (inverse Compton instead of synchrotron) and in addition it might be diluted by thermal radiation at the softer energies.

From the numerous multiwavelength monitorings of 3C 279 we collected the X- and γ -ray data simultaneous with IUE measurements and report in Figure 6 the UV flux at 2000 Å versus the 2 keV X-ray flux (Fig. 6a) and versus the 400 MeV γ -ray flux (Fig. 6b). When simultaneous pairs of SWP and LWP spectra were available, the flux at 2000 Å was obtained from the joint power-law fit of the two spectra (see Tables 2 and 3); otherwise, it was obtained by extrapolating to this wavelength the available flux (Table 1) using the typical spectral index for the corresponding emission level (see Fig. 2; for January 1995, the average spectral index of January 1993 has been used). In 1991, no strictly simultaneous γ -ray and UV data are available, therefore we associated with the EGRET data of June 1991 the IUE measurements of June 1989, based on the similarity of the optical emission state in June 1989 and June 1991 (see Hartman et al. 1996). Both X- and γ -ray emission appears to be generally well correlated with the UV emission, although the X-ray flux

varies somewhat less than the UV, very roughly as the square root of it, as found by a linear regression test, while the γ -ray flux varies roughly as the square of the UV flux. The UV-to-X-ray flux correlated variability between January 1993 and December 1993 is in agreement with this historical trend, in that the X-ray flux increased only by 50%, to be compared to the factor of 3 variation seen in the UV.

On long time scales, these correlations support both the scenario in which the inverse Compton seed photons are the synchrotron photons themselves (synchrotron self-Compton) and that in which the photons upscattered to the highest energies are provided by a source external to the jet, like radiation coming directly from an accretion disk, or reprocessed in a broad line region (external Compton). In the former case, the γ -rays are expected to vary more than the infrared-to-UV flux, due to the non-linearity of the synchrotron self-Compton mechanism (Ghisellini & Maraschi 1996). In the latter case a linear correlation between the optical-UV and the γ -ray flux variations would be expected, but higher amplitude γ -ray variations could be reconciled with this prediction, provided the bulk Lorentz factor of the relativistic plasma varies between the observation epochs (Hartman et al. 1996). Neither scenario can be favored against the other, the relative importance of the two depending on the bulk Lorentz factor (Ghisellini & Maraschi 1996). The largest quasi-simultaneously measured UV and γ -ray fluxes of 3C 279 present an inverted correlation. Although this might be simply due to the non strict simultaneity of the data or to a difference in the physical parameters at the two epochs, like e.g., magnetic field and maximum electron energy (the sampling time is longer than the typical multiwavelength variability time scales), it does not exclude the possibility that, at different epochs, the γ -rays are produced through inverse Compton radiation off optical-UV photons of different origin.

On the shortest time scales (one day or less) the observed variability (the changes in the γ -rays are possibly more than quadratic with respect to UV, Wehrle et al. 1998) is definitely incompatible with external Compton scattering (changes in the bulk Lorentz factor are unlikely to occur on day, or shorter, time scales), and could pose difficulties also for the synchrotron self-Compton model. An alternative is the “mirror” model (Ghisellini & Madau 1996), in which the target photons for the inverse Compton scattering consist of emission line photons produced in a small number of broad line region clouds illuminated by the relativistic jet. The rapid variations caused by the jet on the line emission can result, in the comoving frame of the jet, in more than quadratic variations in the γ -ray flux radiated via the inverse Compton mechanism.

Our proposal of a thermal component underlying the UV continuum of 3C 279 is critical for both ranges of time scales. The UV luminosity we find for the putative accretion disk responsible for this component is consistent with the estimates provided by Dermer

and Schlickeiser (1993) and Sikora et al. (1994), who interpret the high energy spectra of 3C 279 in terms of an inverse Compton scattered isotropic field radiated from a central source, an accretion disk or the broad line region. We recall that the estimated UV luminosity of the accretion disk makes it a reasonable powering source of the Ly α emission line. This line indicates the presence of broad line clouds, some of which could interact with the jet, responsible of the synchrotron continuum, and give rise to the mirror effect. Rapid fluctuations in subcomponents of the Ly α line profile would be expected in this case. Therefore, sensitive UV observations with high spectral resolution would be important for discriminating the active processes. The presence of a thermal component needs to be confirmed by more sensitive UV observations, as well as by more hard X-ray and γ -ray data, during a low state of 3C 279.

We are grateful to C. Cacciari, J. Caplinger, D. De Martino, and N. Loiseau for their assistance with IUE observations and data reduction, and to the IUE staff of Vilspa and GSFC, in particular to W. Wamsteker and Y. Kondo, for their support of this project. We thank R. Scarpa for useful comments to the paper. This work was supported by NASA grants NAG5-2154, NAG5-2538, and NAG5-3138.

REFERENCES

- Aharonian, F., et al. 1997, *A&A*, 327, L5
Bloom, S. D., et al. 1997, *ApJ*, 490, L145
Bonnell, J. T., Vestrand, W. T., & Stacy, J. G. 1994, *ApJ*, 420, 545
Bregman, J. N. 1986, *ApJ*, 301, 708
Bregman, J. N. 1990, *A&AR*, 2, 125
Bregman, J. N. 1994, in *IAU Symp. 159, Multi-Wavelength Continuum Emission of AGN*, ed. T. J.-L. Courvoisier and A. Blecha (Dordrecht: Kluwer), p. 5
Brown, L. M. J., et al. 1989, *ApJ*, 340, 129
Caplinger, J. 1995, *NASA IUE Newsletter No. 55*, 17
Cardelli, J. A., Clayton, G. C., & Mathis, J. S. 1989, *ApJ*, 345, 245
Catanese, M., et al. 1997, *ApJ*, 487, L143
Celotti, A., Maraschi, L., & Treves, A. 1991, *ApJ*, 377, 403
Chiappetti, L., et al. 1999, *ApJ*, 521, in press

- Corbett, E. A., Robinson, A., Axon, D. J., Hough, J. H., Jeffries, R. D., Thurston, M. R., & Young, S. 1996, MNRAS, 281, 737
- Crenshaw, M. D., Bruegman, O. W., & Norman, D. J. 1990, PASP, 102, 463
- Czerny, B., & Elvis, M. 1987, ApJ, 321, 305
- Dermer, C., & Schlickeiser, R. 1993, ApJ, 416, 458
- Edelson, R. A., & Krolik, J. H. 1988, ApJ, 333, 646
- Edelson, R. A., Pike, G. F., Saken, J. M., Kinney, A., & Shull, J. M. 1992, ApJS, 83, 1
- Elvis, M., Lockman, F. J., & Wilkes, B. J. 1989, AJ, 97, 777
- Elvis, M., et al. 1994, ApJS, 95, 1
- Falomo, R., Treves, A., Chiappetti, L., Maraschi, L., Pian, E., & Tanzi, E. G. 1993, ApJ, 402, 532
- Gaidos, J. A., et al. 1996, Nature, 383, 319
- Garhart, M. P., Smith, M. A., Levay, K. L., & Thompson, R. W. 1997, IUE NASA Newsletter No. 57, p.165
- Garhart, M. P. 1998, IUE NASA Newsletter No. 58, in press
- Ghisellini, G., & Maraschi, L. 1996, in “Blazar Continuum Variability”, ASP Conf. Ser., Vol. 110, eds. H. R. Miller, J. R. Webb, and J. C. Noble, p. 436
- Ghisellini, G., & Madau, P. 1996, MNRAS, 280, 67
- Grandi, P., et al. 1996, ApJ, 459, 73
- Grandi, P., et al. 1997, A&A, 325, L17
- Haardt, F., et al. 1998, A&A, 340, 35
- Hartman, R. C., et al. 1992, ApJ, 385, L1
- Hartman, R. C., et al. 1996, ApJ, 461, 698
- Hartman, R. C. 1996, in “Blazar Continuum Variability”, ASP Conf. Ser., Vol. 110, eds. H. R. Miller, J. R. Webb, and J. C. Noble, p. 333
- Imhoff, C. 1996, IUE NASA Newsletter 56, 108
- Imhoff, C. 1997, IUE NASA Electronic Newsletter, Vol. 5, No. 4
- Kolman, M., Halpern, J. P., Shrader, C. R., Filippenko, A. V., Fink, H. H., & Schaeidt, S. G. 1993, ApJ, 402, 514
- Koratkar, A., Pian, E., Urry, C. M., & Pesce, J. E. 1998, ApJ, 492, 173

- Kubo, H., Takahashi, T., Madejski, G., Tashiro, M., Makino, F., Inoue, S., & Takahara, F. 1998, *ApJ*, 504, 693
- Lawson, A., & McHardy, I. M. 1998, *MNRAS*, 300, 1023
- Loiseau, N., & Schartel, N. 1998, <http://ines.vilspa.esa.es/ines/docs/contents.html>
- Macomb, D. J., et al. 1995, *ApJ*, 449, L99
- Makino, F., et al. 1989, *ApJ*, 347, L9
- Maraschi, L., Chiappetti, L., Falomo, R., Garilli, B., Malkan, M., Tagliaferri, G., Tanzi, E. G., & Treves, A. 1991, *ApJ*, 368, 138
- Maraschi, L., Ghisellini, G., & Celotti, A. 1992, *ApJ*, 397, L5
- Maraschi, L., et al. 1994, *ApJ*, 435, L91
- Maraschi, L. 1998, *Nucl. Phys. B (Proc. Suppl.)*, 69/1-3, 389
- Masnou, J. L., Wilkes, B. J., Elvis, M., McDowell, J. C., & Arnaud, K. A. 1992, *A&A*, 253, 35
- Mattox, J. R., Wagner, S. J., Malkan, M., McGlynn, T. A., Schachter, J. F., Grove, J. E., Johnson, W. N., & Kurfess, J. D. 1997, *ApJ*, 476, 692
- Netzer, H. 1990, in *Active Galactic Nuclei, Saas-Fee Advanced Course 20, Lecture Notes 1990*, Swiss Society for Astrophysics and Astronomy, eds. T. J.-L. Courvoisier and M. Mayor (Springer Verlag)
- Netzer, H., et al. 1994, *ApJ*, 430, 191
- Nichols, J. S., & Linsky, J. L. 1996, *AJ*, 111, 517
- Pian, E., et al. 1993, *ApJ*, 486, 784
- Rees, M. J. 1984, *ARAA*, 22, 471
- Rieke, G. H., & Lebofsky, M. J. 1985, *ApJ*, 288, 618
- Sambruna, R. M. 1997, *ApJ*, 487, 536
- Schartel, N., Walter, R., Fink, H. H., & Trümper, J. 1996, *A&A*, 307, 33
- Sembay, S., Warwick, R. S., Urry, C. M., Sokoloski, J., George, I. M., Makino, F., Ohashi, T., & Tashiro, M. 1993, *ApJ*, 404, 112
- Shields, G. A. 1978, *Nature*, 272, 706
- Shrader, C. R., et al. 1994, *AJ*, 107, 904
- Shull, J. M., & Van Steenberg, M. E. 1985, *ApJ*, 294, 599
- Sikora, M., Begelman, M., & Rees, M. J. 1994, *ApJ*, 421, 153

- Takahashi, T., et al. 1996, ApJ, 470, L89
- Thompson, D. J., et al. 1996, ApJS, 107, 227
- Treves, A., et al. 1999, in ASP Conf. Ser. 159, BL Lac Phenomenon, ed L. Takalo (San Francisco: ASP), p. 184
- Ulrich, M.-H., 1981, Space Sci. Rev., 28, 89
- Ulrich, M.-H., Maraschi, L., & Urry, C. M. 1997, ARAA, 35, 445
- Urry, C. M., et al. 1993, ApJ, 411, 614
- Webb, J. R., Carini, M. T., Clements, S., Fajardo, S., Gombola, P. P., Leacock, R. J., Sadun, A., & Smith, A. G. 1990, AJ, 100, 1452
- Wehrle, A. E., et al. 1998, ApJ, 497, 178

Fig. 1.— Multiwavelength light curves of 3C 279 in December 1992-January 1993: (a) dereddened optical R-band fluxes (from Grandi et al. 1996); (b) dereddened IUE fluxes at 2600 Å; (c) de-absorbed fluxes at 1 keV for Galactic $N_{HI} = 2.22 \times 10^{20} \text{ cm}^{-2}$ (from Sambruna 1997). Error bars represent 1- σ uncertainties.

Fig. 2.— De-reddened UV spectra of 3C 279 binned in ~ 100 Å-wide intervals. Like for other synchrotron sources, the spectra steepen with decreasing intensity. However, at the lowest intensity, the spectra are again flat, possibly due to the presence of steady accretion disk emission. Error bars are 1- σ uncertainties. Open symbols represent average IUE spectra for various typical flux levels (see Table 3): the “high” state spectrum (Jul 1988, circles) was obtained by co-addition, weighted with exposure time, of spectra SWP 33864, 33865 for the 1230-2000 Å range and LWP 13566, 13567 for the range 2000-3000 Å; the “medium” state (Jan 1989-May 1992, squares) is the co-addition of SWP 35443, 36420, 42132, 40489, 44806 and LWP 14933, 15677, 20891, 19492, 23207; the “low” state (Dec 1993 and Jan 1996, triangles) has been obtained by co-adding SWP 49681, 49686, 56635 and LWP 31882, 31906, 31908, 31914; the “very low” state (Jan 1993, diamonds) is the co-addition of SWP 46649, 46653, 46657, 46662 and LWP 24652, 24656, 24661, 24665; the stars represent the “extremely low” state observed in January 1995 (SWP 53261). Filled symbols represent HST-FOS spectra in April 1992 (squares) and January 1996 (circles). Superimposed on each representative spectrum is the power-law curve which best fits the data in the interval 1230-2700 Å. Spectral indices are $\alpha = 1.47 \pm 0.02$ (Jul 1988), $\alpha = 1.70 \pm 0.03$ (Jan 1989-May 1992), $\alpha = 1.92 \pm 0.07$ (Dec 1993 and Jan 1996), $\alpha = 0.89 \pm 0.15$ (Jan 1993), $\alpha = 1.65 \pm 0.13$ (HST-FOS 1992), $\alpha = 2.25 \pm 0.04$ (HST-FOS 1996).

Fig. 3.— De-reddened UV flux at 2000 Å versus energy index at the various epochs of IUE and HST observations of 3C 279. The upper branch shows the usual anti-correlation of spectral index and intensity for bright synchrotron sources, while the lower branch suggests the increasing importance of a flat accretion disk component at the lowest UV fluxes.

Fig. 4.— Simultaneous de-absorbed optical-to-X-ray spectral energy distributions of 3C 279 in a faint state, at the four epochs of IUE SWP and LWP observations in January 1993 (see Table 2), and UV-to-X-ray spectral energy distribution in a brighter state, in December 1993 (only the SWP fluxes are simultaneous with the ASCA data, the LWP fluxes are from January 1996, see text). The dotted curve shown in each panel represents the black-body model which best-fits the average UV spectrum of January 1993 ($T = 20000 \pm 1000$ K). The possible disk component is clearly visible in the first four spectra, but disappears when the synchrotron radiation rises. The UV spectral fluxes are binned in ~ 100 Å-wide intervals and the 1- σ uncertainties are estimated as in Falomo et al. (1993). The best fit power-laws to the ROSAT spectra (Sambruna 1997) and ASCA spectrum (0.7-10 keV, this paper) are shown

along with their 90% confidence ranges. The optical data are from Grandi et al. (1996).

Fig. 5.— Amplitude of the Discrete Correlation Function (Edelson & Krolik 1988) between the ROSAT count rates and spectral slopes. The positive time lag corresponds to spectral index changes trailing those of the emission.

Fig. 6.— Historical de-absorbed UV fluxes versus simultaneous (a) X-ray and (b) γ -ray fluxes of 3C 279, on a logarithmic scale. Both panels show clear correlation, with X-rays varying slowly with respect to the UV and γ -rays varying with higher amplitude than the UV. X- and γ -ray points, except the ASCA data of January 1995 which have been analyzed by us, are from Maraschi et al. (1994), Hartman et al. (1996), Hartman (1996), Sambruna (1997), Kubo et al. (1998), Wehrle et al. (1998). The γ -ray data have been converted to Jansky according to Thompson et al. (1996).

Table 1: IUE Observations of 3C 279 in December 1992-January 1996

IUE Image	Observation Midpoint		t ^a	F _λ ^b
	JD - 2,440,000	UT		
LWP 24540	8976.30897	1992 Dec 19.80897	180	0.51 ± 0.07
LWP 24597	8983.14525	26.64525	130	< 0.3 ^c
LWP 24607	8984.15172	27.65172	115	0.51 ± 0.15
LWP 24616	8985.98721	29.48721	156	0.33 ± 0.08
LWP 24640	8988.27792	31.77792	164	0.45 ± 0.07
LWP 24652	8990.28179	1993 Jan 02.78179	360	0.68 ± 0.08
SWP 46649	8990.48576	02.98576	220	1.24 ± 0.15
SWP 46653	8991.05085	03.55085	600	1.08 ± 0.10
LWP 24656	8991.38942	03.88942	360	0.58 ± 0.06
SWP 46657	8992.05343	04.55343	660	0.82 ± 0.11
LWP 24661	8992.41147	04.91147	360	0.57 ± 0.07
SWP 46662	8993.05675	05.55675	660	1.03 ± 0.15
LWP 24665	8993.43048	05.93048	315	0.56 ± 0.08
LWP 24699	8998.23747	10.73747	150	0.56 ± 0.07
SWP 49681	9346.15726	Dec 24.65726	200	2.42 ± 0.21
SWP 49686	9347.04185	25.54185	330	3.49 ± 0.21
SWP 53261	9720.84844	1995 Jan 03.34844	280	0.67 ± 0.17
SWP 56635	10107.94094	1996 Jan 25.44094	325	2.46 ± 0.16

^a Exposure time in minutes.

^b Observed average flux in the range 1650-1850 Å for SWP spectra and 2500-2700 Å for LWP spectra. Units are 10⁻¹⁵ erg s⁻¹ cm⁻² Å⁻¹.

^c 3-σ upper limit.

Note. Errors represent 1-σ uncertainties.

Table 2: Fit Parameters of De-reddened Spectra^a

UT ^b (Jan 1993)	02.88378	03.72014	04.73245	05.74362
α^c (1230-2700 Å)	1.37 ± 0.18	0.75 ± 0.13	0.60 ± 0.16	1.17 ± 0.16
F^d (mJy)	0.139 ± 0.007	0.153 ± 0.006	0.145 ± 0.008	0.147 ± 0.007
χ^2_ν (N_{dof})	1.55 (499)	1.72 (513)	1.64 (513)	2.07 (513)
α^e_{INES} (1230-2700 Å)	1.53 ± 0.18	1.51 ± 0.13	1.90 ± 0.15	1.13 ± 0.18
F^f_{INES} (mJy)	0.19 ± 0.01	0.210 ± 0.008	0.212 ± 0.008	0.17 ± 0.01
χ^2_ν (N_{dof})	1.11 (499)	1.31 (513)	1.11 (513)	1.41 (513)
α (1230-8000 Å)	1.52 ± 0.04	1.62 ± 0.04	1.64 ± 0.04	1.76 ± 0.05
χ^2_ν (N_{dof})	5.21 (11)	3.76 (12)	4.07 (12)	2.61 (12)
α (2400-8000 Å)	1.82 ± 0.06	1.91 ± 0.06	1.91 ± 0.07	2.06 ± 0.09
χ^2_ν (N_{dof})	0.94 (5)	1.39 (5)	2.07 (5)	1.27 (5)
α (4400-8000 Å)	1.88 ± 0.08	1.80 ± 0.09	1.78 ± 0.08	1.96 ± 0.11
χ^2_ν (N_{dof})	1.32 (2)	0.29 (2)	0.38 (2)	0.05 (2)
T^g_{BB} (K)	17000 ± 800	20000 ± 1000	22000 ± 1400	17800 ± 850
F^h_{BB} (mJy)	0.16 ± 0.08	0.17 ± 0.07	0.15 ± 0.09	0.16 ± 0.08
χ^2_ν (N_{dof})	1.52 (499)	1.67 (513)	1.62 (513)	2.03 (513)

^a The NEWSIPS extracted IUE spectra have been used, unless otherwise indicated. Reduced χ^2 values, with relative number of degrees of freedom in parentheses, refer to the fit parameters preceding them.

^b Observation midpoint of quasi-simultaneous SWP and LWP spectra (see Table 1).

^c Fitted power-law index ($F_\nu \propto \nu^{-\alpha}$).

^d Fitted power-law normalization at 2000 Å.

^e Power-law index fitted to INES extracted IUE spectra.

^f Power-law normalization fitted to INES extracted IUE spectra at 2000 Å.

^g Fitted black-body temperature.

^h Fitted black-body normalization at 2000 Å:

$$F_{BB} = N \left(\frac{\nu}{\nu_0} \right)^3 [\exp(h\nu/kT) - 1]^{-1}, \quad N = 2\pi h \nu_0^3 \Sigma / c^2, \quad \text{where}$$

Σ = angular size of the emitting region in steradians, and $\nu_0 = 1.5 \times 10^{15}$ Hz.

Note. Errors represent 1- σ uncertainties.

Table 3: IUE Final Archive Merged Spectra of 3C 279:
Power-Law Fit Parameters^a

Spectral Pair		Date	α_{UV}	χ^2_ν	$\alpha_{UV,0}$	F_ν^b (mJy)	χ^2_ν
SWP	LWP						
33864	13566	1988 Jul 06	1.76 ± 0.02	1.52	1.63 ± 0.03	3.69 ± 0.05	1.47
33865	13567	1988 Jul 06	1.51 ± 0.03	1.89	1.36 ± 0.03	3.91 ± 0.06	1.89
35443	14933	1989 Jan 29	1.61 ± 0.03	1.28	1.47 ± 0.03	1.72 ± 0.03	1.30
36420	15677	1989 Jun 09	1.85 ± 0.02	1.80	1.70 ± 0.02	2.15 ± 0.03	1.79
40489	19492	1990 Dec 30	1.97 ± 0.02	1.68	1.83 ± 0.02	2.34 ± 0.03	1.66
42132	20891	1991 Jul 27	2.07 ± 0.03	1.40	1.92 ± 0.03	1.54 ± 0.02	1.38
44806	23207	1992 May 29	1.80 ± 0.04	1.82	1.65 ± 0.04	1.51 ± 0.02	1.81
56635	31908	1996 Jan 25	2.31 ± 0.09	1.49	2.16 ± 0.09	0.40 ± 0.01	1.48

^a Results for both observed (col. 4) and de-reddened spectra (cols. 6 and 7) are given along with their respective reduced χ^2 (cols. 5 and 8).

^b De-reddened fitted flux at 2000 Å. The interstellar extinction $A_V = 0.13$ implies, at this wavelength, a correction of $\sim 40\%$ with respect to the observed flux.

Note. Errors represent 1- σ uncertainties.

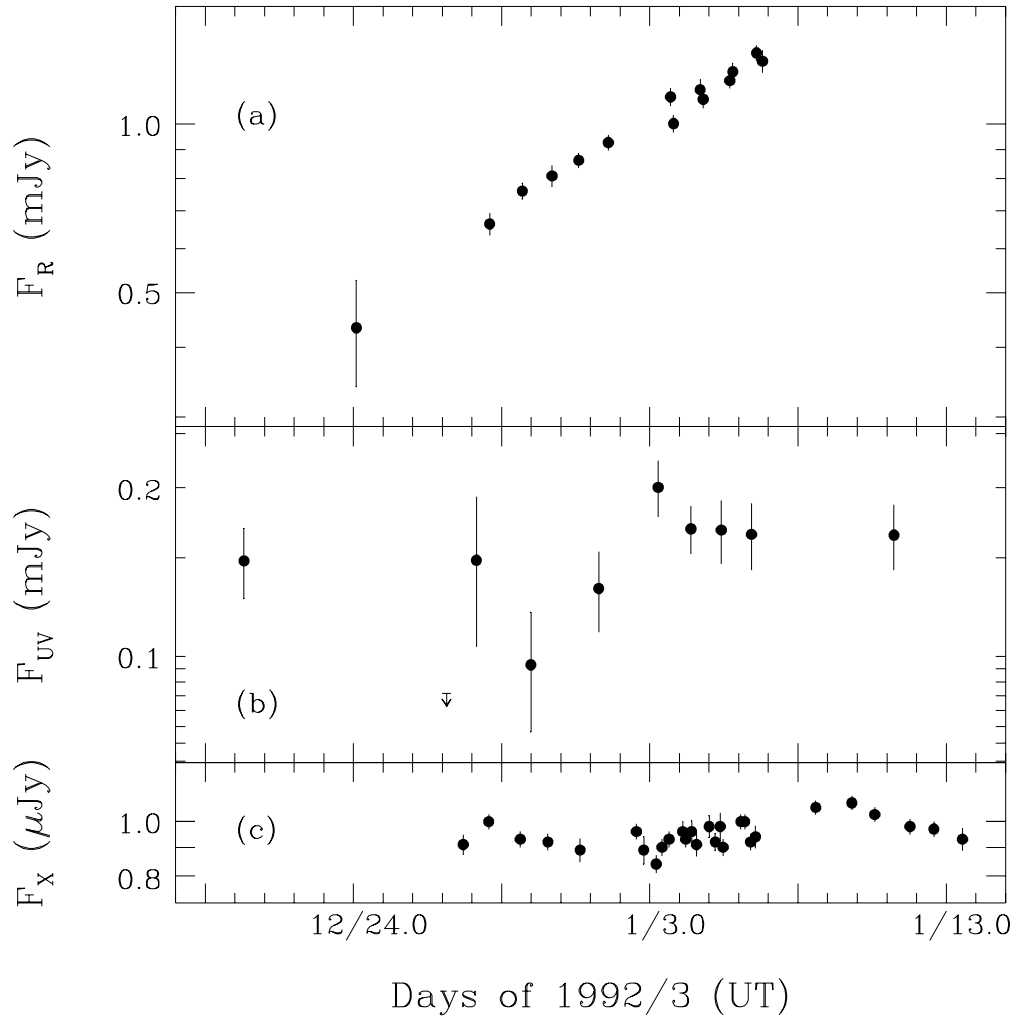


Fig. 1

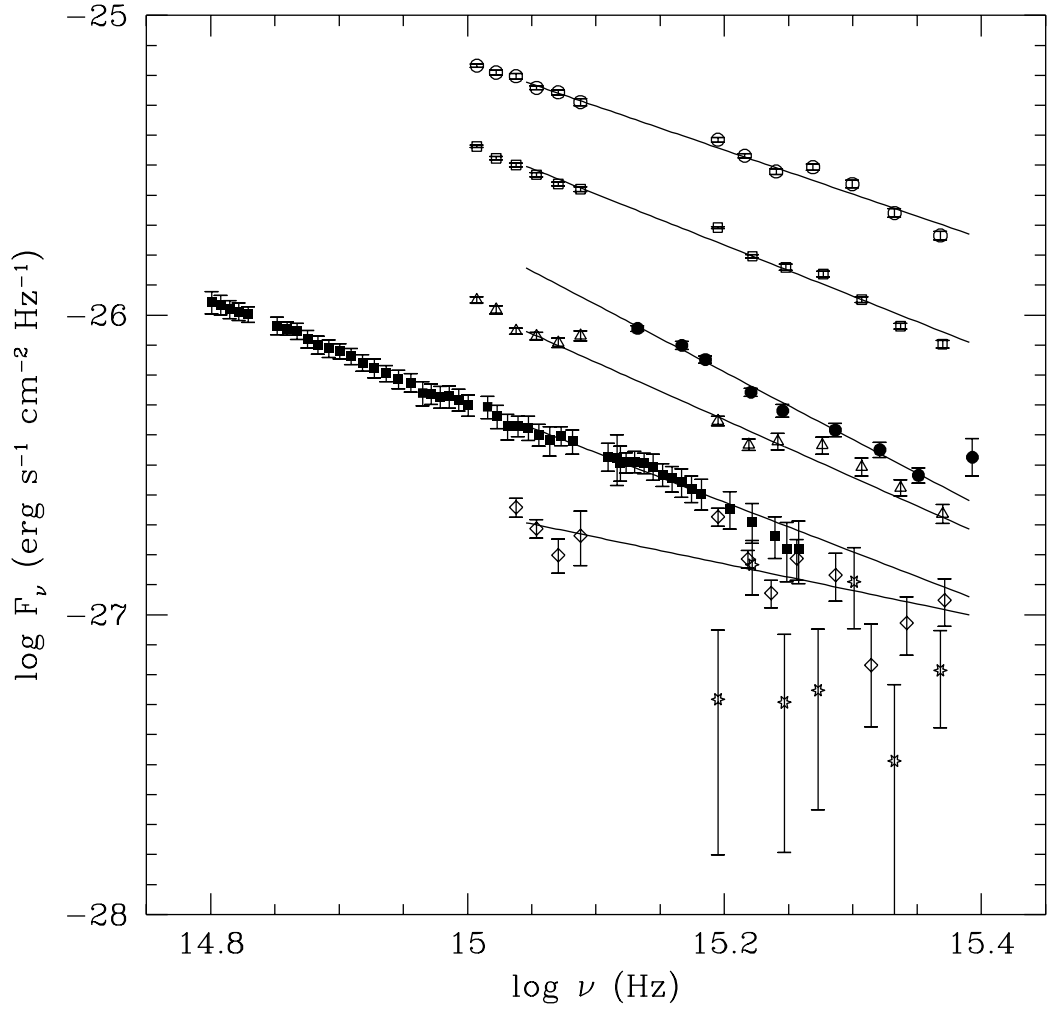


Fig. 2

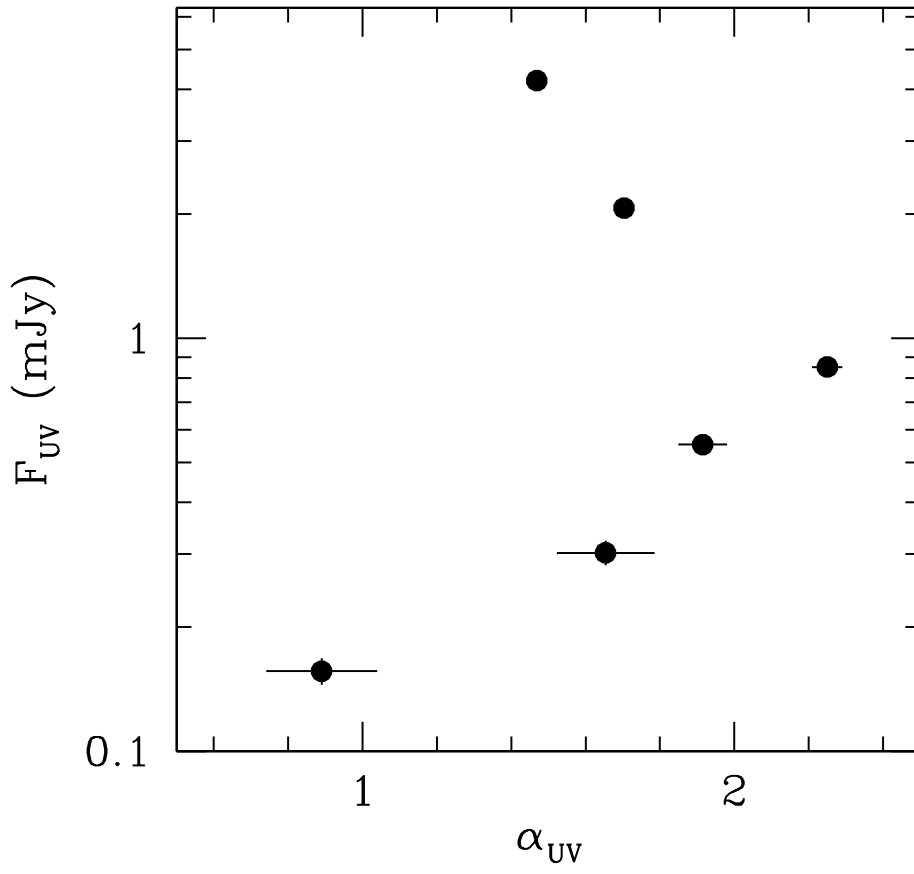


Fig. 3

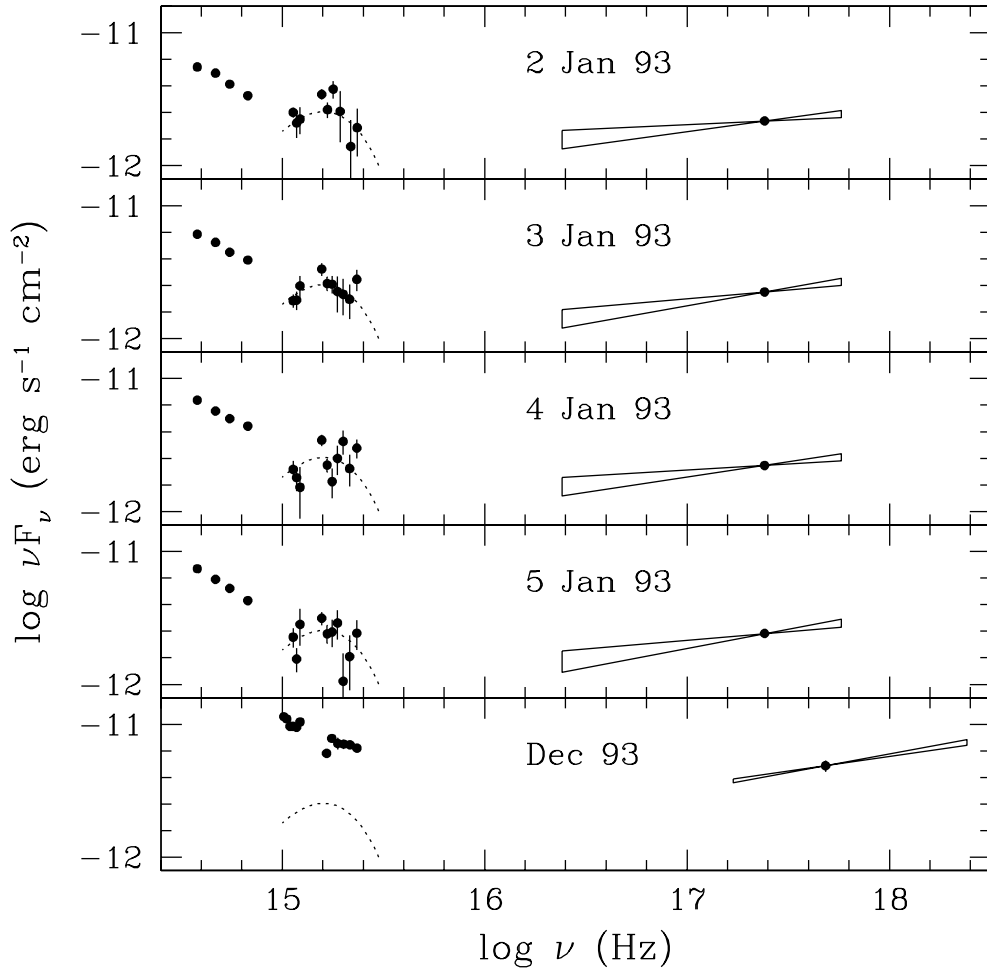


Fig. 4

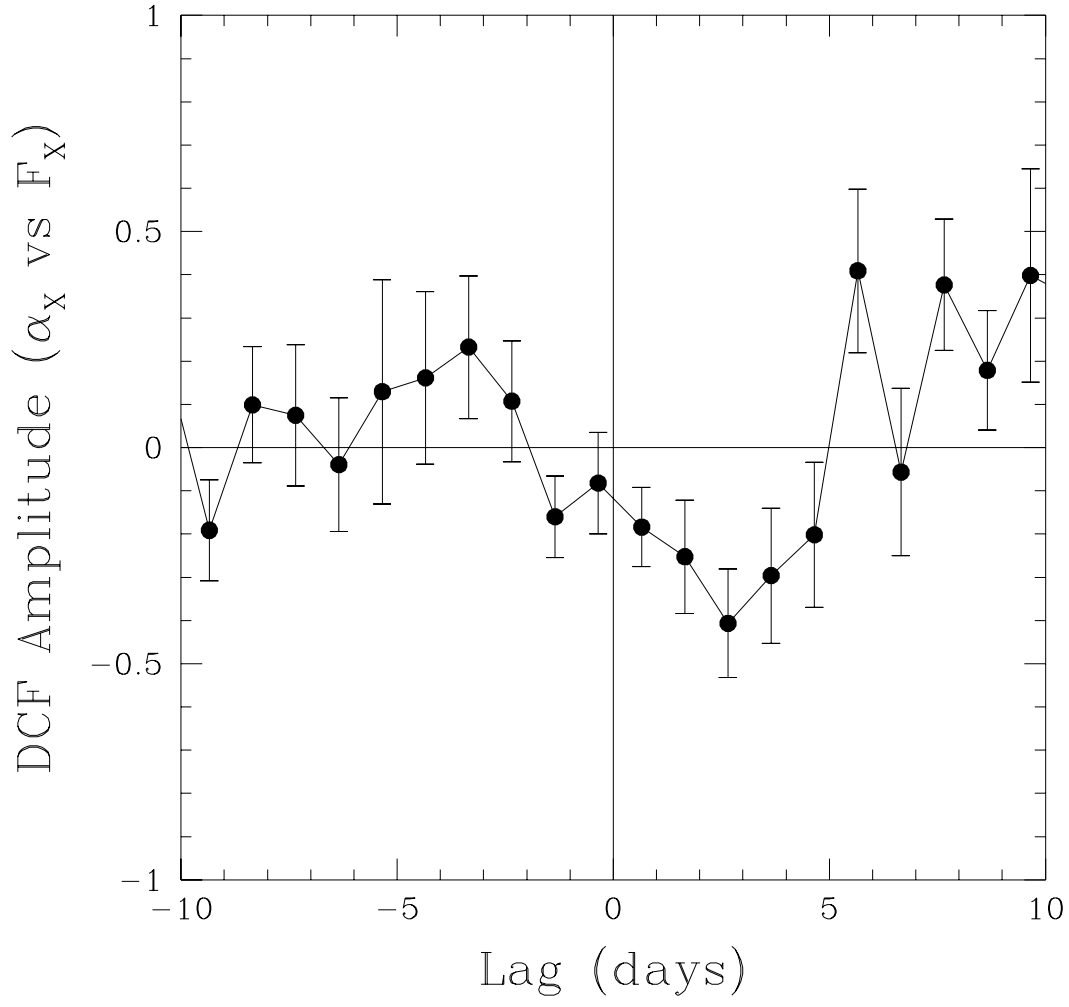


Fig. 5

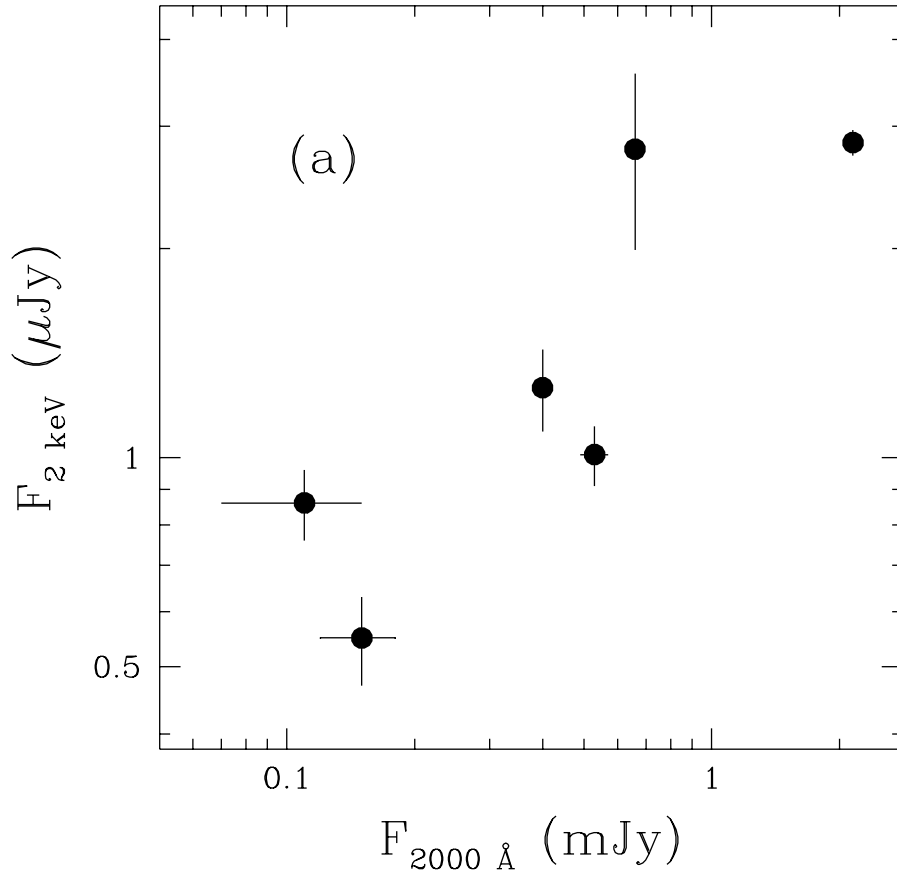


Fig. 6a

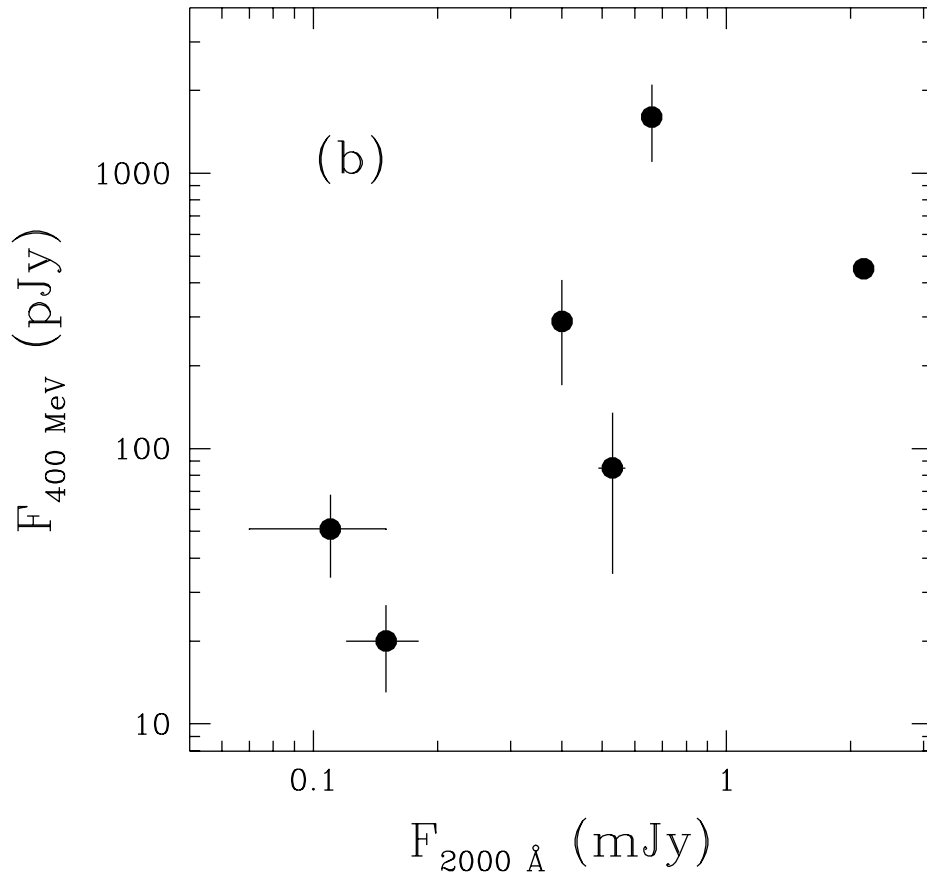


Fig. 6b